Bulletin of the Seismological Society of America, Vol. 105, No. 2b, pp. –, , doi: 10.1785/0120140183

Thermal Condition of the 27 October 2012 M_w 7.8 Haida Gwaii Subduction Earthquake at the Obliquely Convergent Queen Charlotte Margin

by Kelin Wang, Jiangheng He, Franziska Schulzeck, Roy D. Hyndman, and Michael Riedel

Abstract The 2012 M_w 7.8 Haida Gwaii earthquake confirmed very oblique subduction and slip partitioning at the southern Queen Charlotte margin. In this study, we re-examine the thermal regime near the earthquake using new model constraints and with the recognition that hydrothermal circulation in the subducting oceanic crust can significantly affect the margin thermal regime. The observed heat flow values are extremely high just seaward of the trench but decrease rapidly landward. We explain this pattern as the consequence of very vigorous hydrothermal circulation in the subducting oceanic crust. Using a finite-element model, we simulate the thermal effect of the circulation using a high-conductivity proxy that represents a very high Nusselt number in an aquifer along the top of the oceanic plate. Our thermal model indicates that the temperature at the intersection of the megathrust and the strike-slip Queen Charlotte fault (QCF) just seaward of the coast is about 350° C, approximately the limit of seismogenic behavior, and cooler than previous models that did not include hydrothermal circulation. The change of plate motion kinematics across the QCF approximately coincides with a down-dip transition of the thermally controlled seismogenic behavior of the megathrust. Seaward of the QCF, the shallow megathrust accommodates mainly the margin-normal component of relative plate motion, with the strike-slip component accommodated by the QCF. This portion of the megathrust exhibits stick slip and produced the 2012 Haida Gwaii earthquake. Landward of the QCF, the megathrust fully accommodates the very oblique motion of the oceanic plate beneath the continental crust and exhibits creep.

Introduction

The Queen Charlotte margin is primarily a dextral transcurrent continent–ocean boundary of the North America (NA) and Pacific (PA) plates (Fig. 1a). Along the southern portion of this margin, in the region of Haida Gwaii (formerly named Queen Charlotte Islands), relative motion of the two plates has had a small convergent component of ~20° at 15–20 mm/yr over the past ~6 million years (Hyndman and Hamilton, 1993; Atwater and Stock, 1998). On 27 October 2012, an M_w 7.8 thrust earthquake occurred offshore of Haida Gwaii (Fig. 1) that generated a substantial tsunami (Leonard and Bednarski, 2014). Its shallow-thrust focal mechanism nearly orthogonal to the margin strongly supports the view that the convergent component of NA–PA motion in this area is presently accommodated by PA subducting beneath NA along a recently developed megathrust (e.g., James *et al.*, 2013; Lay *et al.*, 2013).

In a study of seismic structure and thermal regime of Haida Gwaii, Smith *et al.* (2003) developed thermal models to investigate whether surface heat flow observations were consistent with the subduction of PA underneath NA (see also Smith, 1999). They concluded that the broad pattern of heat flow observations were slightly more consistent with the subduction model than with a model in which convergence is consumed by internal deformation of the two plates. In addition to more structural data and better understanding of the tectonic regime of the area, two primary reasons motivated us to reinvestigate the thermal regime of Haida Gwaii.

1. The 2012 Haida Gwaii earthquake is an example of megathrust rupture due to the subduction of a very young and warm oceanic plate. The age of the subducting PA plate is only 6–8 Ma, similar to that of the subducting Juan de Fuca plate along the Cascadia subduction zone to the south. Based on the subduction model of Smith *et al.* (2003), the deeper part of the Haida Gwaii rupture would have occurred where the model temperature is about 450° C or higher, warmer than commonly understood for the nucleation of subduction earthquakes. It is important

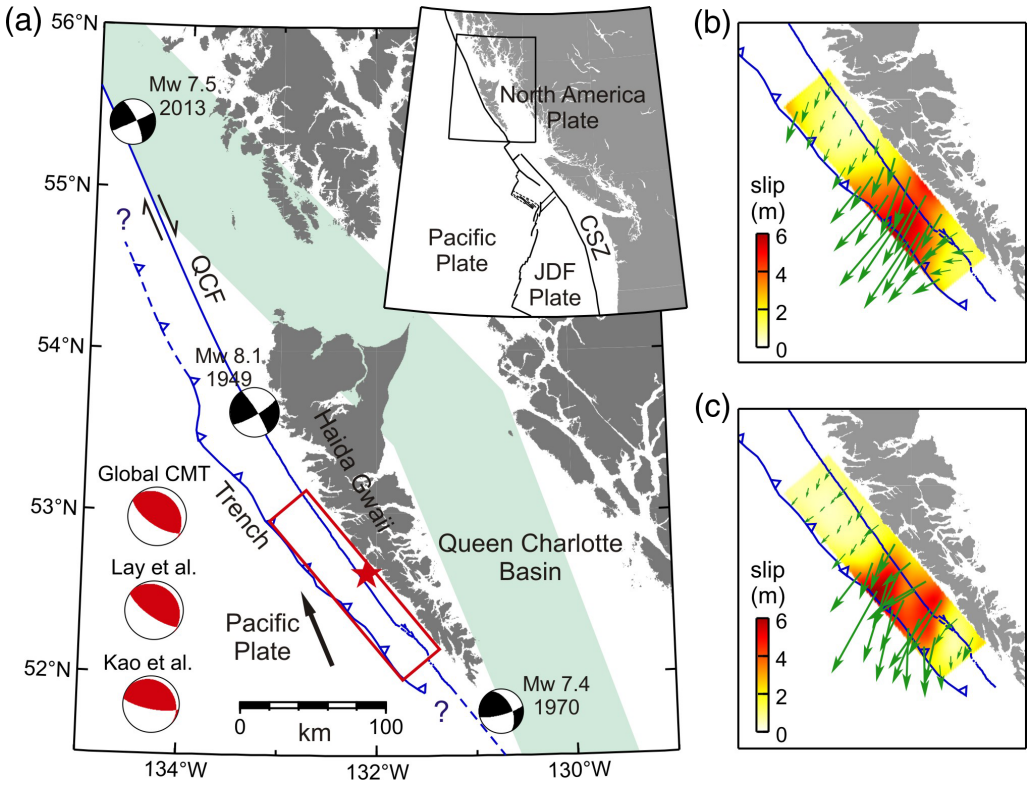

Figure 1. Regional tectonics and the 2012 Haida Gwaii earthquake. (a) Tectonics of the Queen Charlotte margin and large historical earthquakes. Inset shows plate boundaries of a larger area and the location of the map area. QCF, Queen Charlotte fault; CSZ, Cascadia subduction zone. Strike-slip component of the Pacific plate motion with respect to North America is accommodated mainly by the QCF. The small convergent component is accommodated by subduction at the trench. Shaded region shows range of possible position of the leading edge of the subducting slab based on various assumptions of subduction history and kinematics as summarized in Smith *et al.* (2003). Star shows the epicenter of the 2012 M_w 7.8 Haida Gwaii earthquake determined by Kao *et al.* (2015). Beach balls are moment tensor solutions by Global Centroid Moment Tensor, Lay *et al.* (2013), and Kao *et al.* (2015). Rectangle is the rupture area in the models shown in (b) and (c). Focal mechanism of the 2013 earthquake is from Lay *et al.* (2013), and those for the 1949 and 1970 events are from Rogers (1982). (b) Slip vectors (arrows) and magnitude (shading) of a rupture model determined by nonlinear inversion of GPS data using the finite-fault model of Lay *et al.* (2013) as the starting model. (c) Similar to (b) but using the U.S. Geological Survey finite-fault model as the starting model. The models in (b) and (c) are described in Nykolaishen *et al.* (2015). The color version of this figure is available only in the electronic edition.

to re-examine the thermal condition of the rupture zone. A better definition of the thermal condition of the Haida Gwaii rupture helps to better understand the seismogenic zone, especially its down-dip limit, at Cascadia and other warm-slab subduction zones.

2. Recent recognition of the thermal effect of hydrothermal circulation in subducting crust allows us to take a fresh look at the thermal regime in this area. There are some very high heat flow values seaward of the Queen Charlotte Trough that are much higher than that expected for the age of the oceanic crust. Smith *et al.* (2003) did not address these high values and took the heat flow expected for the age of crust as the seaward boundary condition of their model. Spinelli and Wang (2008) recently demonstrated that similarly high heat flows in one area of the Nankai subduction zone, southwest Japan, also accompanied with a very rapid landward decrease, could be well explained by vigorous hydrothermal convection in the subducting young oceanic crust. In this study, we investigate whether the same process applies to Haida Gwaii.

In this work, we compile new and previously published structural information to define the geometry of the megathrust and subducting slab and develop a 2D thermal model for the Haida Gwaii region. We will show that by including the effect of vigorous hydrothermal circulation in the subducting crust and using the newly defined plate geometry, the model can very well explain heat flow observations in this area and the thermally controlled down-dip limit of the rupture of the 2012 earthquake. We will discuss how the thermal results help us understand the rheology and slip behavior of the megathrust.

Oblique Convergence Tectonics and the 27 October 2012 Earthquake

At the southern Queen Charlotte margin (Fig. 1a), the PA plate moves relative to NA at ~50 mm/yr in a northwesterly

direction, 15°–20° oblique to strike. The strike-slip Queen Charlotte fault (QCF) is at a short distance off the coast, bisecting the continental shelf. Surface morphology, especially that from multibeam sonar bathymetry (Barrie *et al.*, 2013), clearly indicates the QCF's modern almost purely strike-slip motion. To the north, the strike of the QCF gradually becomes more parallel with the direction of PA–NA motion (Fig. 1a). Even farther north, the extension of the QCF, the Fairweather fault, extends 1000 km into southern Alaska to the Alaska subduction zone. The central part of the QCF hosted the M_w 8.1 Queen Charlotte earthquake of 1949, the M_w 7.5 earthquake of 2013, and many other events as discussed by Rogers (1986). Most large earthquakes are of strike-slip mechanisms, but smaller events along the southern part of the Haida Gwaii margin indicate oblique convergence (e.g., Bird, 1997; Ristau *et al.*, 2007).

A small amount of recent crustal shortening is indicated in Hecate Strait seismic reflection data to the east (e.g., Rohr and Dietrich, 1992), but we conclude that most convergence is across the west coast of the islands. The Global Positioning System (GPS) vectors on Haida Gwaii are 10°–30° from the margin trend, and earthquake mechanisms indicate current oblique convergence. A number of models have been suggested for how the convergence is accommodated (e.g., Dehler and Clowes, 1988; Prims *et al.*, 1997; Rohr *et al.*, 2000; Smith *et al.*, 2003), but with new information from a variety of sources, the case for underthrusting is clear (see Hyndman, 2015). A key prediction of the subduction model is the presence of a mature megathrust that may cause large subduction earthquakes and tsunamis (Smith *et al.*, 2003; Leonard *et al.*, 2012). A number of small earthquakes with shallow thrust mechanisms have been recorded in this area (Bird, 1997), but the M_w 7.8 Haida Gwaii earthquake of 2012 has provided the most direct evidence for the presence of a subduction type megathrust and therefore validated the subduction model (James *et al.*, 2013).

Slip vectors of finite-fault models constrained by seismic waveform data (e.g., Lay *et al.*, 2013; G. Hayes, U.S. Geological Survey, personal comm., 2012) are oriented predominantly orthogonal to the margin. Coseismic displacements of GPS sites also are largely trench normal (Nykolaishen *et al.*, 2015), indicating predominantly margin-normal thrust motion. Slip vectors shown in Figure 1b,c were obtained by using these GPS data to update the seismological finite-fault models. The lack of significant coseismic uplift based on post-event field surveys (Haeussler *et al.*, 2015) and the coseismic subsidence of a GPS site very near the coast (Nykolaishen *et al.*, 2015) support the conclusion that the rupture zone was mostly offshore, and likely mainly seaward of the QCF. This general slip pattern strongly supports the model of slip partitioning (Hyndman and Hamilton, 1993; Smith *et al.*, 2003), that is, the strike-normal and strike-parallel components of relative plate motion are accommodated by the shallowly dipping megathrust beneath the Queen Charlotte Terrace and the subvertical QCF, respectively.

The megathrust and the QCF define a wedge-shaped sliver, the Queen Charlotte Terrace accretionary prism, that translates along strike to the northeast. The distance from the trench to the surface trace of the QCF is only about 30 km (Fig. 1a). The sliver is much narrower than the fore-arc sliver that is commonly seen at oblique subduction zones, which includes fore-arc crust (e.g., Fitch, 1972; McCaffrey, 1994), but it is not unique. For example, the narrow sliver at the Puysegeur (or Fjordland) subduction zone of southern New Zealand that serves to partition oblique convergence onto the megathrust and the southernmost segment of the Alpine fault is of a similar size (Beavan *et al.*, 2010). We have investigated the thermal condition of the megathrust seaward and landward of its intersection with the QCF and how the thermal condition influences the megathrust's seismogenic behavior.

Thermal Model

Heat Flow Constraints

There are limited heat flow data across the Haida Gwaii margin, and as we noted above, the heat flow in Hecate Strait to the east of the islands is affected by mid-Tertiary extension. However, the data are adequate to provide constraints for underthrusting thermal models. Hyndman *et al.* (1982) conducted seafloor heat flow measurements west of Haida Gwaii using marine heat flow probes and also obtained a land value in the Tasu area near the west coast from 11 shallow (< 300 m) boreholes in a small area (Fig. 2a). Yorath and Hyndman (1983) reported preliminary heat flow values obtained from deep (> 2730 m) industry exploration wells in the Queen Charlotte Sound east of Haida Gwaii. Values from these wells were included in a summary of heat flow measurements in the Canadian Cordillera (Lewis, 1991) and the global heat flow database (Pollack *et al.*, 1993). However, these heat flow values were reassessed using more data from these wells, and the revised values were reported by Lewis *et al.* (1991). Lewis *et al.* (1991) also reported more heat flow values based on marine probe measurements from the Masset Inlet and a few locations in the Queen Charlotte Sound and some values from land boreholes (Fig. 2a). Similar to Smith *et al.* (2003), we use the values from Hyndman *et al.* (1982) and the compilation of Lewis *et al.* (1991).

When projected onto a margin-normal transect (Fig. 2b), the most remarkable feature of the heat flow distribution is a rapid landward decrease from very high values (> 240 mW/m^{-2}) seaward of the trench to much lower values (50–70 mW/m^{-2}) over a distance of only 20–30 km. The very high values are much higher than expected from an oceanic plate of age 8 Ma and were not used as model constraints in the study of Smith *et al.* (2003), and the sharp landward decrease cannot be explained by typical subduction models (Wada and Wang, 2009; Gao and Wang, 2014). In the Model Results and Discussion section, we will demonstrate that these high values and the rapid landward decrease can be explained by the effect of vigorous hydrothermal circulation within the subducting crust.

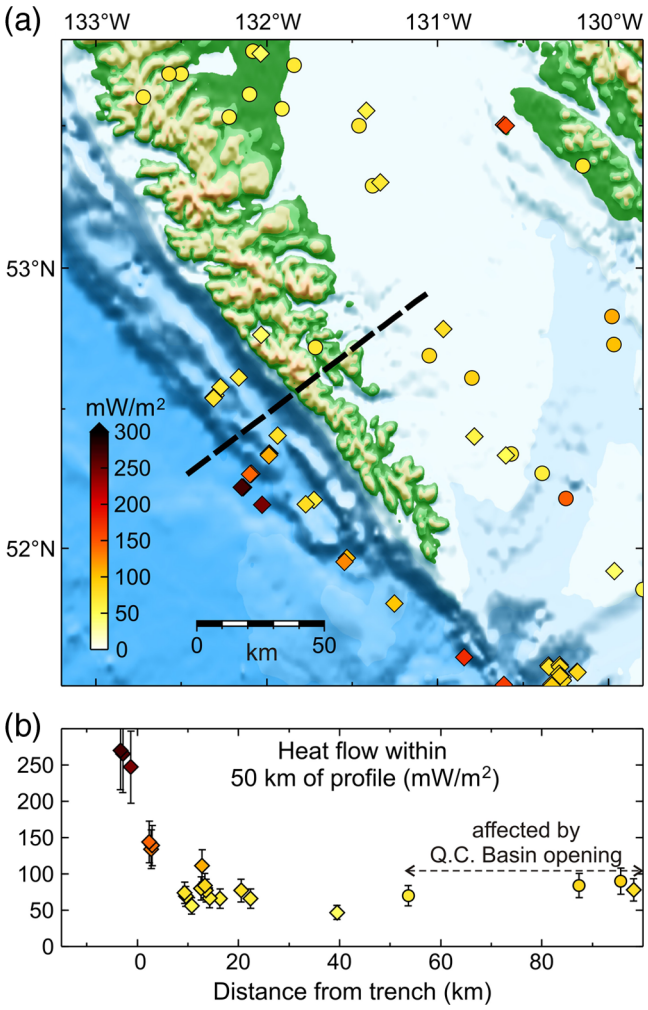

Figure 2. Heat flow observations reported by Hyndman *et al.* (1982; diamonds) and Lewis *et al.* (1991; circles). (a) Map view of heat flow sites and values. Thick dashed line shows the model profile of this work. (c) Heat flow data from within 50 km of the model profile. All heat flow values are assigned an uncertainty of 20%. A few tens of kilometers away from the trench, the thermal regime is increasingly influenced by the recent extension of the Queen Charlotte Basin. The color version of this figure is available only in the electronic edition.

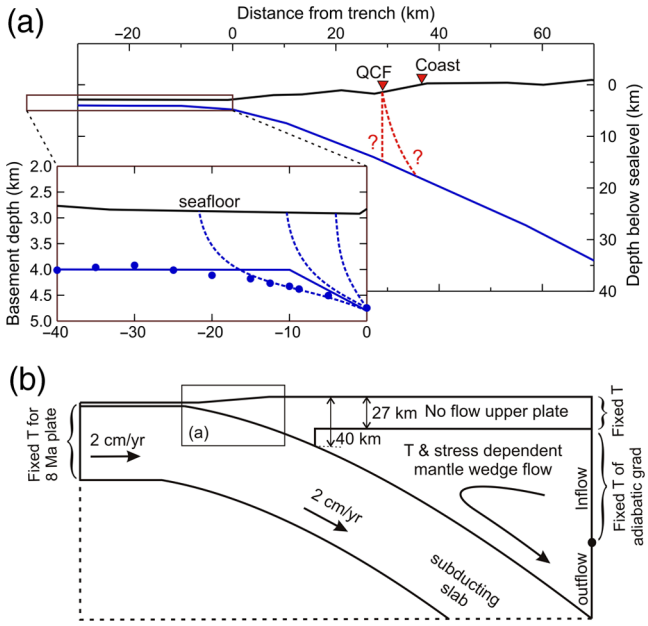

Figure 3. Model setup. (a) Interface geometry used in this work. The dip of the QCF is poorly known, and two possibilities are shown (dashed lines with question marks). Inset shows the sediment interface geometry of the incoming plate. Solid circles are interface depth based on interpretation of seismic survey data. Dashed lines show different hypothetical scenarios of how the megathrust may breach the seafloor. The simplified geometry (solid line) is used in our model. (b) Schematic illustration of model structure and boundary conditions (not to scale). Details of the mantle wedge rheology can be found in Wada and Wang (2009). Temperature (T) along the crust segment of the landward boundary follows a conductive gradient, and the inflow part of the mantle segment follows an adiabatic gradient (Wada and Wang, 2009). The color version of this figure is available only in the electronic edition.

Lewis *et al.* (1991) concluded that the average heat flow of the Queen Charlotte basin to the east of the islands (Fig. 1a) is 70 ± 6 mW/m^{-2}. The Queen Charlotte basin is only about 100–200 km from the trench, and for a mature subduction zone, this would be the cold fore-arc with heat flows of 30–50 mW/m^{-2} (Wada and Wang, 2009). The observed warm state is due to mid-Tertiary crustal extension (Yorath and Hyndman, 1983; Rohr and Dietrich, 1992; Hyndman and Hamilton, 1993), and we have not attempted to model the heat flow data in this region (Fig. 2b).

Geometry of the Plate Interface

Based on seismic receiver function and offshore seismic reflection definition of the underthrusting plate, we conclude that the plate geometry does not vary significantly along strike in this area. We therefore construct an average geometry of subduction interface across the margin of southern Haida Gwaii for the thermal model. From about 50–90 km landward of the trench, the interface geometry is relatively well constrained by receiver function analysis of teleseismic waves (Smith *et al.*, 2003; Bustin *et al.*, 2007). The analysis showed the interface beneath Haida Gwaii to be dipping east to reach a depth range of 25–40 km (Fig. 3a).

A number of previous surveys and analyses have estimated sediment thickness of 1–1.5 km seaward of the trench, thickening in the Terrace accretionary prism (Hyndman and Ellis, 1981; Dehler and Clowes, 1988; Mackie *et al.*, 1989; Spence and Long, 1995). These observations and conclusions have been confirmed by new multichannel seismic surveys conducted two months after the 2012 Haida Gwaii earthquake (Fig. 3a) (Riedel *et al.*, 2014). The points in Figure 3a (inset) are based on five trench-normal survey profiles. To convert travel time to depth, we have assumed an average P wavespeed of 2500 m/s for the sediment. Exactly where the plate interface begins, that is, how the megathrust breaches the seafloor, is not known, because there are no clear images

of frontal thrusts. Figure 3a (inset) shows a few hypothetical scenarios, all involving frontal thrusts. We use the simplified geometry shown in Figure 3a to approximate crudely the effect of likely frontal thrusts. In this geometry, the plate interface increases its dip rather abruptly at 10 km seaward of the trench. As described in the Model Results and Discussion section, numerical tests show that this abrupt increase, as well as hydrothermal circulation in the subducting crust, is necessary for explaining the sharp heat flow gradient across the trench (Fig. 2b).

There is little survey information on the interface geometry between the trench and about 50 km landward. All five survey profiles used for Figure 3a extend much farther landward through the epicenter of the Haida Gwaii earthquake, but the basement reflector is too deep to be clearly discerned landward of the trench because of the small air gun source used. The plate interface that hosted the 2012 Haida Gwaii earthquake was not clearly imaged in previous seismic surveys either. Some previous structural models did not have a slab. Similar to Smith *et al.* (2003) and Bustin *et al.* (2007), we fill the gap between the trench and the receiver function results by assuming that the plate interface is smooth and that its dip increases monotonically with depth.

Aftershocks of the Haida Gwaii earthquake form a band dipping shallowly to the northeast. From events that are large enough to yield centroid moment tensor solutions ($M_w > 4.3$), the focal mechanisms are predominantly normal faulting, with a distinct lack of shallow thrust events (Farahbod and Kao, 2015). Therefore these aftershocks are most likely within the subducting crust. The plate interface shown in Figure 3a is consistent with this distribution of aftershocks.

Because of the uncertainties in the dip of the QCF, there are some uncertainties in the depth of its intersection with the megathrust. Two possibilities are shown in Figure 3a. The possibility of the QCF dipping steeply to the east arises because three large strike-slip earthquakes along this fault (1949, 1970, and 2013) feature a steeply easterly dipping fault plane (Fig. 1a). Based on these possibilities, we estimate that the QCF intersects the megathrust in the depth range of 15–20 km.

As explained by Smith *et al.* (2003), the location of the leading edge of the subducting slab depends on the time when subduction was initiated and the position of the Juan de Fuca–PA–NA triple junction at that time (Fig. 1a). The short history of subduction and consequently the short slab length is the reason for the lack of a volcanic arc and Wadati–Benioff seismicity. It also implies a small mantle wedge. The short slab and very oblique subduction must also give rise to a complex 3D pattern of mantle flow different from the typical corner flow in subduction zone mantle wedges (Wada and Wang, 2009).

Modeling Method and Parameters

Similar to Smith *et al.* (2003), we develop a 2D steady-state model along a representative strike-normal transect (Fig. 3b). Our model is not designed to model the recent extension of the Queen Charlotte basin and the associated complex mantle flow pattern. Therefore, our domain of interest is rather small, a few tens of kilometers landward of the trench and shallower than 30 km, although the model mesh is several times as large in both dimensions. Although subduction is very oblique, the thermal gradient in the strike direction in this shallow part must be negligibly small when compared with those in the strike-normal and depth directions. Therefore a 2D representation of the thermal field is reasonable.

The thermal time constant for a 30 km rock column is about 7 Ma (assuming diffusivity of 10^{-6} m^2/s). This is similar to the ~8 Ma duration of subduction in this region (Atwater and Stock, 1998). The maximum thickness of the sliver west of the QCF is of the order of 15–20 km, with a thermal time constant around 2 Ma. The time evolution of the thermal regime since subduction initiation can thus be ignored in our region of interest. If the age, and hence thermal structure, of the incoming plate arriving at the trench changes with time, so will the thermal state of the subduction zone (Wang *et al.*, 1995). Off Haida Gwaii, seafloor magnetic lineations are at a small angle with the strike direction (Wilson, 1988), and the subduction direction relative to the fore-arc sliver is roughly margin normal because of the slip partitioning discussed above. As a result, the age change of the subducting plate at a given location of the fore-arc sliver is extremely slow. For these reasons, the assumption of steady state is reasonable.

We use the finite-element code PGCtherm2D written by J. He. Our modeling strategy is a combination of those used by Wada and Wang (2009) and Spinelli and Wang (2008). The model consists of an upper plate, a subducting plate, and a viscous mantle wedge in between (Fig. 3b). Physical property values assumed for various units of the system are shown in Table 1. These values are similar to what was used and explained in previous thermal modeling work for the Cascadia margin (e.g., Hyndman and Wang, 1993). The subducting plate is assigned a rate of 2 cm/yr, roughly the margin-normal component of the PA–NA motion. A change of 0.5 cm/yr has little effect on the results. The mantle wedge has a temperature- and stress-dependent power law rheology with parameters appropriate for wet olivine (Wada and Wang, 2009). The part of the upper plate shallower than the reported average Moho depth of 27 km in this area (Spence and Long, 1995) is assigned zero velocity, but the actual thickness of the no-flow upper plate is greater and is controlled by the mantle wedge rheology. The landward vertical boundary is assigned geotherms that yield surface heat flow 70 mW/m^{-2} at distances corresponding to the Queen Charlotte basin. The upper boundary (seafloor and ground surface) is assigned 0° C temperature.

The temperature profile along the vertical seaward boundary represents the age-dependent thermal state of the incoming plate (Fig. 3b). This temperature profile is advected down-dip by the downgoing slab and governs the thermal budget of our domain of interest. The ~1 km thick sediment section on the incoming plate has two competing effects. Recent and fast sedimentation has a cooling effect, but the low

Table 1
Thermal Parameters Used in Modeling

Thermal Unit	Thermal Conductivity ($W\,m^{-1}\,K^{-1}$)	Thermal Capacity ($MJ\,m^{-3}\,K^{-1}$)*	Heat Production ($\mu W\,m^{-3}$)
Sediment	2.0	N/A†	1.3
Continental upper crust	2.5	N/A†	1.3
Continental lower curst	2.5	N/A†	0.4
Mantle wedge	3.1	3.3	0.02
Oceanic lithosphere	2.9	3.3	0.02

*Volumetric thermal capacity is specific heat times density.
†Not required for steady-state modeling.

conductivity of the sediment has an insulating and thus warming effect (Wang and Davis, 1992). Because the sedimentation history is poorly known, the net thermal effect of the sediment cover cannot be constrained. However, because the sediment cover is thin, its thermal effect if any will have little impact on the thermal state of the subduction system more than 10 km from the trench. We thus use the GDH1 model of the cooling of the oceanic plate without sedimentation (Stein and Stein, 1992) to model the temperature profile of the incoming plate. As will be evident from the ensuing section, any uncertainties due to the neglect of the sedimentation effect will be overshadowed by the large effect of hydrothermal circulation in the subducting crust. We set the model boundary to be 80 km seaward of the trench and use a 1D temperature profile for a 4 Ma old plate for this boundary. The flat portion of the incoming plate continues to cool as it moves toward the trench. With a 2 cm/yr convergence rate, the plate age becomes 8 Ma when it arrives at the trench. The reason why we need to put the seaward boundary of the model a large distance from the trench will be explained in the subsection Hydrothermal Circulation in Subducting Crust.

The thermal, petrologic, and volcanic processes of mature subduction zones are controlled by a sharp transition in the state of coupling between the subducting slab and the mantle wedge. Globally, the down-dip transition from decoupling to coupling occurs at a depth of 70–80 km (Wada and Wang, 2009). However, as described in the two preceding sections, the slab–mantle wedge system at Haida Gwaii is not yet fully developed and is affected by additional warming due to the recent extension of the Queen Charlotte basin. In particular, the stagnant and cold region of the wedge corner is expected to be underdeveloped and small. We assume the no-flow part of the wedge corner overlies only the shallower than 40 km part of the subduction interface (Fig. 3b). Based on numerical testing, making the no-flow part larger will underpredict heat flow observations in the Queen Charlotte basin but has no effect on the model results seaward of the QCF.

Our past experience indicates that the value of the effective coefficient of friction of the plate interface μ', which accounts for both the intrinsic friction and the effect of pore fluid pressure, is about 0.03 (e.g., Wang and Suyehiro, 1999; Currie *et al.*, 2002; Wada and Wang, 2009; Gao and Wang, 2014). Here, we employ a similar value, but we will conduct sensitivity tests to illustrate the effects of using other values.

Model Results and Discussion

Hydrothermal Circulation in Subducting Crust

Buoyancy driven vigorous hydrothermal convection in young igneous oceanic crust is well recognized, even under a low-permeability sediment seal that prevents thermally significant fluid ventilation through the seafloor. Davis *et al.* (1997) reported unambiguous evidence for such sealed circulation in the igneous crust of the Juan de Fuca ridge flank, where the convection is so vigorous that the sediment-basement interface is kept isothermal. Spinelli and Wang (2008) reasoned that such circulation should continue after the young crust enters a subduction zone, provided that the permeability remains high. The vigor of the circulation may even be enhanced if the permeability is increased due to fracturing caused by the bending of the subducting plate. This continuing circulation serves to mine heat from greater depths and dump it at the trench, causing the surface heat flow to be very high at the trench but to decrease rapidly landward. Using this mechanism, Spinelli and Wang (2008) explained the heat flow observations from the Muroto area of the Nankai subduction zone, southwest Japan.

The heat flow pattern at Haida Gwaii, with very high values seaward of the trench and a steep landward decrease (Fig. 2), is remarkably similar to what is observed at Nankai. We therefore apply the method of Spinelli and Wang (2008) to Haida Gwaii. We assume extremely efficient convective heat transfer within an aquifer along the top of the subducting crust. The efficiency of convective heat transfer in the aquifer is characterized by the Nusselt number Nu, defined as the ratio of the total heat transferred through the aquifer to the heat that would be transferred by conduction alone in the absence of convection. The thermal effect of the hydrothermal circulation is thus modeled using a conduction proxy, that is, in a model of heat conduction but with the effective thermal conductivity of the aquifer increased by a factor of Nu (Davis *et al.*, 1997; Spinelli and Wang, 2008). The high Nu simulates the thermal effects of efficient mixing that transports heat from the hotter, deeper part of the subduction zone to the shallow, trench region. We assume this aquifer to be 1000 m thick, but there is trade-off between this thickness and Nu. The same thermal effect can be produced by a thinner aquifer of higher Nu or a thicker aquifer of lower Nu. Because of the high conductivity in this layer, the seaward boundary of the model is set to be far from the trench as described in subsection Modeling Method and Parameters, otherwise the fixed temperature along this boundary would affect the near-trench results (Spinelli and Wang, 2008).

Surface heat flow measurements and subsurface temperatures predicted by our preferred model are shown in Figure 4a,b, respectively. In this model, Nu is uniformly 1000 along the aquifer that extends throughout the length

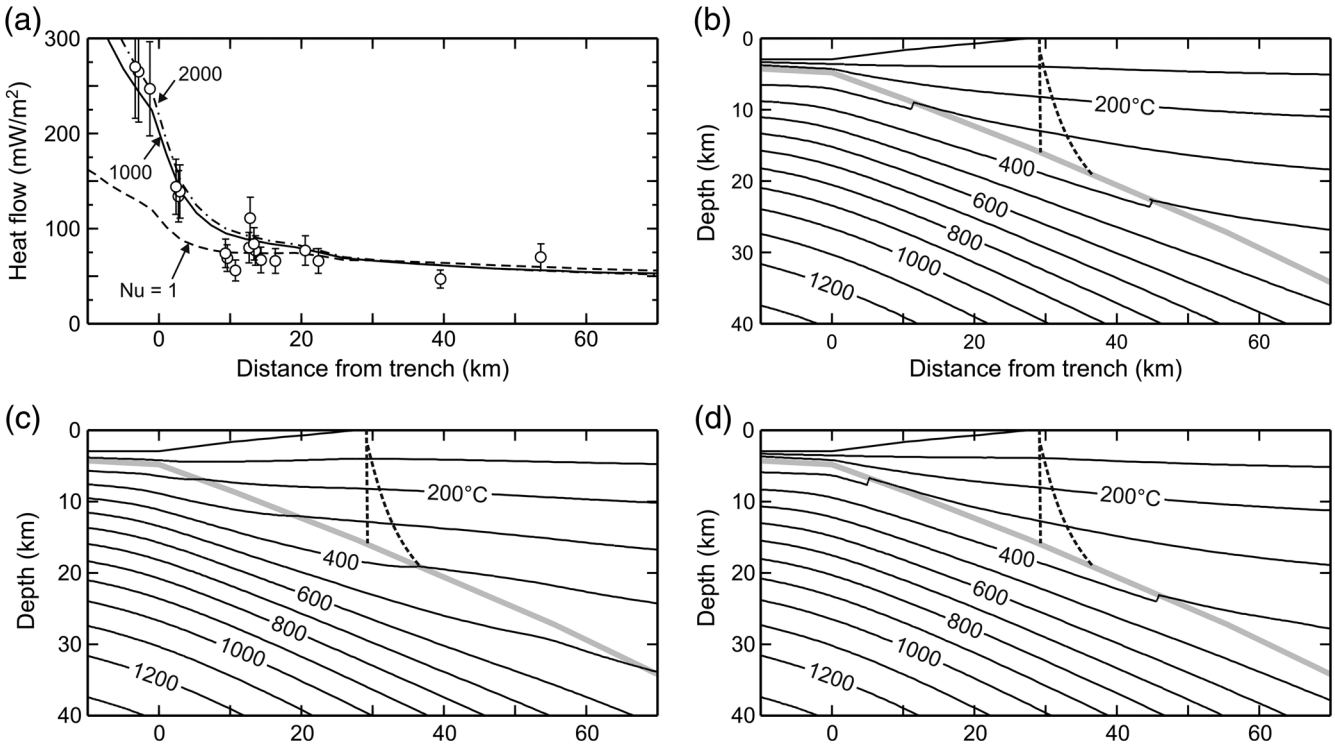

Figure 4. Model results. (a) Model predicted surface heat flow for the preferred model assuming vigorous hydrothermal circulation in the subducting crust (Nu = 1000), for a model of no circulation (Nu = 1), and for a model of extremely vigorous circulation (Nu = 2000). In all these models, the effective friction coefficient of the fault is 0.03. (b,c,d) Subsurface temperatures of the preferred model, the model of no circulation (Nu = 1), and the model of extremely vigorous circulation (Nu = 2000), respectively. Two possible geometries of the QCF are shown by dashed lines. Results toward the northeast boundary of the shown model domain (right side) should be used with caution, because this model does not address the effect of the recent extension of the Queen Charlotte Basin (Fig. 2b).

of the subducting plate in the model and $\mu' = 0.03$. For comparison, in Figure 4 we also show results for a model of Nu = 1 (no hydrothermal circulation) and Nu = 2000 (more extreme circulation).

The vigor of hydrothermal convection is described by the Rayleigh number Ra, and the relationship between Ra and Nu can be empirically established based on laboratory experiments and numerical modeling (e.g., Wang, 2004). Because Ra is proportional to permeability, the permeability value can be inferred from Nu through the known Ra–Nu relation. However, Ra also depends on temperature-dependent fluid properties such as density and viscosity, so that the same high Nu requires a higher permeability at lower temperatures than at higher temperatures. If we follow the reasoning of Spinelli and Wang (2008), a Nu of 1000 requires a permeability of 10^{-10}–10^{-9} m^2 at and seaward of the trench but diminishing values with increasing depth (and thus temperature) landward of the trench. Assuming the aquifer permeability decreases exponentially with increasing depth results in a nearly uniform Nu (Spinelli and Wang, 2008), especially in the shallow part of the model within our domain of interest. Conversely, a uniform permeability assigned to the aquifer leads to dramatic down-dip increase in locally derived Nu values. Although the two approaches cause little difference to predicted heat flow, Spinelli and Wang (2008) prefer the model of decreasing permeability because of expected permeability reduction due to increasing confining pressure with depth. Here, we are content with using a uniform Nu to represent the thermal effect of vigorous convection and refrain from inferring further details of the convection system and permeability distribution. The reason is that some of the important factors required by such inferences are very poorly known, such as the actual thickness of the aquifer and its change with depth, the Ra–Nu relationship, and mathematical quantification of how Nu, a number designed to characterize heat transfer normal to the aquifer, represents the thermal effects of convective mixing along the aquifer.

The very vigorous circulation within the subducting crust is consistent with the highly fractured state and hence high permeability of the incoming crust. Many fractures are seen in seismic images collected from the postearthquake cruise (Riedel *et al.*, 2014), and the rather sharp bending of the plate as it enters the subduction zone (Fig. 3a) should cause more fractures. Numerous normal-faulting aftershocks of the Haida Gwaii earthquake have been recorded around the trench area (Farahbod and Kao, 2015). They indicate the presence of faults and fractures deep inside the subducting plate. Patches of materials of high seismic wavespeed in the frontal wedge of the upper plate may be interpreted to be the results of pieces of the subducting basaltic crust accreted to

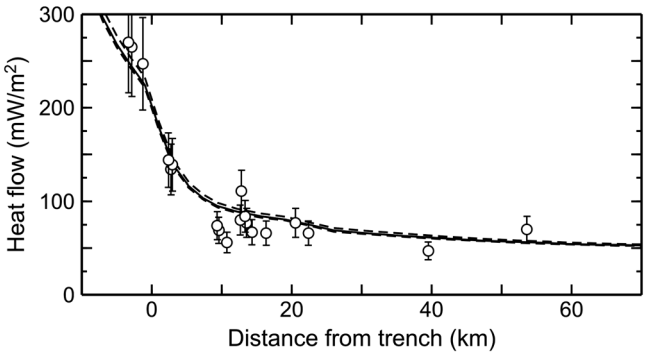

Figure 5. Test results showing the negligible effect of using different values of effective friction coefficient μ' for the megathrust for a model of Nu = 1000. Solid line is the preferred model ($\mu' = 0.03$; Fig. 4a). The two dashed lines are for models with no frictional heat (slightly colder) and with strong frictional heating ($\mu' = 0.1$).

the upper plate (Riedel *et al.*, 2014), again indicating the fractured state of the subducting crust. If the aquifer that hosts the hydrothermal convection is much thicker than 1000 m, a Nusselt number much less than 1000 can produce the thermal effect delivered by the preferred model.

Frictional Heating

In modeling the shallow thermal regime of subduction zones, the most critical yet uncertain parameter is usually the friction coefficient of the plate interface that determines the amount of frictional heating (Gao and Wang, 2014). In comparison, effects of uncertainties in other parameters such as thermal conductivities, heat production, and subduction rate, etc. become very small. In our model, however, the effect of frictional heating is small, and it is the effect of hydrothermal circulation discussed above that dominates the results and uncertainties. In Figure 5, we show heat flow values predicted by a model with no frictional heating and a model with friction heat three times the preferred value of $\mu' = 0.03$, in comparison with the preferred model. Because frictional heat is efficiently carried away from the fault by the vigorous hydrothermal circulation, these models produce similar results.

Thermal Control of the Thrust-Fault Seismogenic Zone

The thermal modeling results can help us understand how temperatures may control the seismogenic behavior of the megathrust. Slip partitioning at Haida Gwaii is schematically shown in Figure 6. In this conceptual model, the motion of the shallow segment of the megathrust seaward of the QCF is nearly margin normal because of slip partitioning. Landward of the QCF, there is no slip partitioning, and the slab is subducting very obliquely. In the models shown in Figure 4, the temperature of the megathrust around its intersection with the QCF is about 350° C, colder than the results of Smith *et al.* (2003) by 50° C–100° C mainly because of our incorporation of hydrothermal cooling of the subducting crust. If the QCF is vertical, the temperature at the intersection is not very sensitive to the assumed vigor of hydrothermal circulation in the subducting crust. If the QCF dips landward, the temperature of the intersection is about 400° C in the absence of hydrothermal circulation (Fig. 4c) but colder in the presence of the circulation such as in the preferred model shown in Figure 4b.

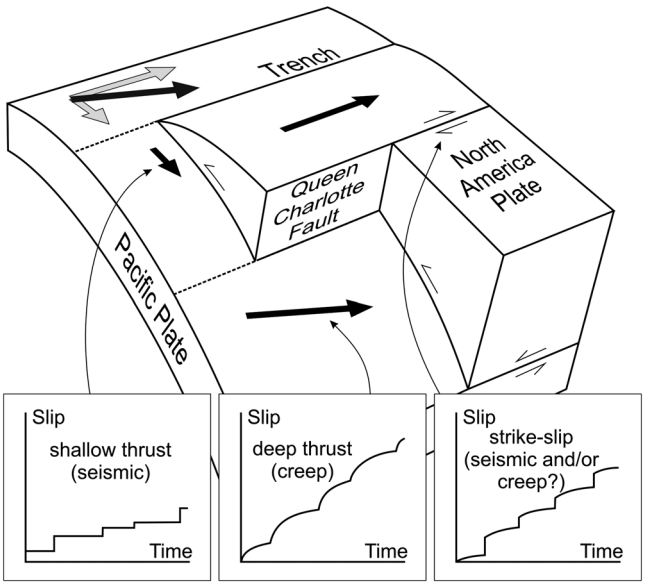

Figure 6. Thermally based conceptual model of slip partitioning in the Haida Gwaii region. The fore-arc sliver bounded by the megathrust and QFC travels along the margin. The shallow and colder ($T < 350°$ C) megathrust seaward of QFC accommodates plate convergence, exhibits stick-slip thrust motion, and produced the 2012 M_w 7.8 earthquake. There is no slip partitioning landward of QFC, and the deeper megathrust is warmer and expected to creep in a highly oblique direction, with the rate of motion affected by seismic slip of the shallow megathrust. QFC accommodates the strike-slip component of PA–NA motion and is cold enough for stick-slip motion.

Based on the arguments of Hyndman and Wang (1993) and Hyndman *et al.* (1997), the seismogenic zone of subduction megathrusts tends to be limited by a temperature of 350° C. Above 350° C, the fault tends to strengthen with increasing slip rate and hence inhibits earthquake nucleation, but coseismic slip may extend some distance into this regime. The models in Figure 4 show that seaward of the QCF where the plate interface undergoes mostly thrust motion because of slip partitioning, the thermal condition facilitates seismic slip. Landward of the QCF where slip is not partitioned, the thermal condition tends to inhibit seismic slip. Although coseismic slip may dynamically propagate some distance landward of the QCF, this deeper part of the megathrust is expected to exhibit mostly creep behavior. A creeping megathrust landward of the QCF not only explains why the 2012 Haida Gwaii rupture was confined to be mostly seaward of the QCF but also is consistent with the fact that landward of the QCF no thrust events have ever been identified that can be associated with the plate interface.

Therefore, we propose that the change from slip partitioning to no partitioning across the QCF corresponds approximately to the change in the slip behavior of the megathrust, from seismic slip to creep, as illustrated by two of the insets in Figure 6. We speculate that the location of the QCF may be related to the thermal condition. The shallower stick-slip segment of the megathrust spends most of its time being locked and sustains greater stress, but the deeper creeping segment sustains much lower stress. With very oblique subduction, the contrast in strength and slip behavior of the megathrust may have promoted localization of dextral shear of the overriding plate at the location of the QCF over the geological history. Slip partitioning requires that the total shear traction along the basal thrust of the fore-arc sliver be large enough to overcome the frictional strength of the strike-slip fault and any other resistance to the margin-parallel motion of the sliver. The observed slip partitioning at Haida Gwaii indicates that the stronger stick-slip shallow segment of the megathrust seaward of the QCF meets this condition.

On the basis of thermal considerations alone, the QCF is sufficiently cold to permit stick-slip behavior. There are other factors that can cause a cold fault to creep (Wang and Bilek, 2014). Historical seismicity (Rogers, 1986) (Fig. 1a) shows the QCF to be seismogenic in general. The Haida Gwaii segment has not produced a significant earthquake in the era of instrumental recording, although it may have been responsible for some of the aftershocks of the 1949 M_w 8.1 earthquake (Rogers, 1986). Hyndman and Weichert (1983) concluded that the historical seismicity on the QCF fault zone has a seismic moment rate that indicates the fault moves almost entirely seismically. As well, the GPS data on the islands appear to require that the QCF be nearly completely locked (e.g., Mazzotti *et al.*, 2003). We therefore suggest that this segment is a seismic gap to be filled by a future strike-slip earthquake.

Conclusions

We have developed a 2D finite-element model to investigate the thermal environment of the 2012 M_w 7.8 thrust earthquake at the extremely obliquely convergent Haida Gwaii margin. The model is designed to study the relatively shallow part of the thrust fault from the trench to several tens of kilometers landward and does not address the mid-Tertiary extension of the Queen Charlotte basin farther east. Based on the model results shown in Figure 4 and the numerous numerical tests not displayed in this article, we draw the following conclusions.

1. The very high heat flow values just seaward of the trench that previous thermal modeling efforts did not address and the very rapid landward decrease in heat flow can both be explained by the effect of vigorous hydrothermal circulation within the subducting oceanic crust, for which there is evidence at other subduction zones. The circulation serves to transport heat from larger depths to the trench area. The very high permeability required by the vigorous circulation is consistent with the fractured state of the subducting plate inferred from seismic reflection observations and extensional aftershocks of the 2012 earthquake.
2. The rapid landward decrease in heat flow also requires an abrupt onset of a geometrical effect that is represented in the model by abrupt increases in the dip of the plate interface around the trench. Seaward of the trench, this increase may partially account for the effects of potential frontal thrusts. Overall, the sharp bending of the slab reflected by the dip increase is consistent with the numerous normal-faulting earthquakes around the trench and the fractured state of the subducting plate.
3. The shallow part of the megathrust seaward of its intersection with the QCF is cooler than 350° C, explaining its seismogenic behavior. The deeper part landward of the QCF beneath the islands is warmer and is expected to exhibit mostly creep behavior. The transition from slip partitioning to no partitioning across the QCF is therefore accompanied with a change in the seismogenic behavior of the megathrust.

Data and Resources

Heat flow data shown in Figure 2 have all been published in references cited in the article and can be obtained from the first author upon request. The thermal modeling code used in this work was written by J. He. Figures were generated with the help of the Generic Mapping Tool (Wessel and Smith, 1995).

Acknowledgments

A scholarship offered by the German Academic Exchange Service enabled F. S. to visit the Pacific Geoscience Centre to conduct the initial part of the modeling work. We thank T. Sun for assistance in compiling information on subduction interface geometry used in our modeling. The manuscript benefitted from comments from two anonymous reviewers and Guest Editor T. James. This is Geological Survey of Canada contribution 20140106.

References

Atwater, T., and J. Stock (1998). Pacific-North America Plate Tectonics of the Neogene Southwestern United States: An update, *Int. Geol. Rev.* **40,** 375–402.

Barrie, J. V., K. W. Conway, and P. T. Harris (2013). The Queen Charlotte fault, British Columbia: Seafloor anatomy of a transform fault and its influence on sediment processes, *Geo. Mar. Lett.* **33,** 311–318, doi: 10.1007/s00367-013-0333-3.

Beavan, J., S. Samsonov, P. Denys, R. Sutherland, N. Palmer, and M. Denham (2010). Oblique slip on the Puysegur subduction interface in the 2009 July M_w 7.8 Dusky Sound earthquake from GPS and InSAR observations: Implications for the tectonics of southwestern New Zealand, *Geophys. J. Int.* **183,** 1265–1286.

Bird, A. L. (1997). Earthquakes in the Queen Charlotte Islands region: 1982–1996, *Master's Thesis*, School of Earth and Ocean Sciences, University of Victoria, Canada.

Bustin, A. M. M., R. D. Hyndman, H. Kao, and J. F. Cassidy (2007). Evidence for underthrusting beneath the Queen Charlotte Margin, British Columbia, from teleseismic receiver function analysis, *Geophys. J. Int.* **171,** 1198–1211.

Currie, C. A., R. D. Hyndman, K. Wang, and V. Kostoglodov (2002). Thermal models of the Mexico subduction zone: Implications for the megathrust seismogenic zone, *J. Geophys. Res.* **107,** 2370, doi: 10.1029/2001JB000886.

Davis, E. E., K. Wang, J. He, D. Chapman, H. Villinger, and A. Rosenberger (1997). An unequivocal case for high Nusselt number hydrothermal convection in sediment-buried igneous oceanic crust, *Earth Planet. Sci. Lett.* **146,** 137–150.

Dehler, S. A., and R. M. Clowes (1988). The Queen Charlotte Islands refraction project. Part I. The Queen Charlotte Fault Zone, *Can. J. Earth Sci.* **25,** 1857–1870.

Farahbod, A., and H. Kao (2015). Spatiotemporal distribution of aftershocks during the first week of the 2012 Haida Gwaii aftershock sequence, *Bull. Seismol. Soc. Am.* **105,** doi: 10.1785/0120140173.

Fitch, T. J. (1972). Plate convergence, transcurrent faults and internal deformation adjacent to southeast Asia and the western Pacific, *J. Geophys. Res.* **77,** 4432–4460.

Gao, X., and K. Wang (2014). Strength of stick-slip and creeping subduction megathrust from jheat flow observations, *Science* **345,** 1038–1041.

Haeussler, P., R. Witter, and K. Wang (2015). Intertidal biological indicators of coseismic deformation of the M 7.8 Haida Gwaii, Canada, earthquake, *Bull. Seismol. Soc. Am.* **105,** doi: 10.1785/0120140197.

Hyndman, R. D. (2015). Tectonics and structure of the Queen Charlotte Fault Zone, Haida Gwaii, and large thrust earthquakes, *Bull. Seismol. Soc. Am.* **105,** doi: 10.1785/0120140181.

Hyndman, R. D., and R. M. Ellis (1981). Queen Charlotte fault zone: Microearthquakes from a temporary array of land stations and ocean bottom seismographs, *Can. J. Earth Sci.* **18,** 776–788.

Hyndman, R. D., and T. S. Hamilton (1993). Queen Charlotte area Cenozoic tectonics and volcanism and their association with relative plate motions along the northeastern Pacific Margin, *J. Geophys. Res.* **98,** 14,257–14,277.

Hyndman, R. D., and K. Wang (1993). Thermal constraints on the zone of najor thrust earthquake failure: The Cascadia Subduction Zone, *J. Geophys. Res.* **98,** 2039–2060.

Hyndman, R. D., and D. H. Weichert (1983). Seismicity and rates of relative motion on the plate boundaries of western North America, *Geophys. J. Int.* **72,** 59–82.

Hyndman, R. D., T. J. Lewis, J. A. Wright, M. Burgess, D. S. Chapman, and M. Yamano (1982). Queen Charlotte fault zone: Heat flow measurements, *Can. J. Earth Sci.* **19,** 1657–1669.

Hyndman, R. D., M. Yamano, and D. A. Oleskevich (1997). The seismogenic zone of subduction thrust faults, *Isl. Arc* **6,** 244–260.

James, T., G. C. Rogers, J. C. Cassidy, H. Dragert, R. D. Hyndman, L. Leonard, L. Nykolaishen, M. Riedel, M. Schmidt, and K. Wang (2013), Field studies target 2012 Haida Gwaii earthquake, *Eos Trans. AGU* **94,** no. 22, 197–198.

Kao, H., S.-J. Shan, and A. Farahbod (2015). Source characteristics of the 2012 Haida Gwaii earthquake sequence, *Bull. Seismol. Soc. Am.* **105,** doi: 10.1785/0120140165.

Lay, T., L. Ye, H. Kanamori, Y. Yamazaki, K. F. Cheung, K. Kwong, and K. D. Koper (2013). The October 28, 2012 M_w 7.8 Haida Gwaii underthrusting earthquake and tsunami: Slip partitioning along the Queen Charlotte Fault transpressional plate boundary, *Earth Planet. Sci. Lett.* **375,** 57–70.

Leonard, L. J., and J. Bednarski (2014). Field survey following the 28 October 2012 Haida Gwaii tsunami, *Pure Appl. Geophys.* **171,** doi: 10.1007/s00024-014-0792-0.

Leonard, L. J., G. C. Rogers, and S. Mazzotti (2012), A preliminary tsunami hazard assessment of the Canadian coastline, *Geol. Surv. Can. Open-File 7201*, 126 pp., doi: 10.4095/292067.

Lewis, T. J. (1991). Heat flux in the Canadian Cordillera, in *Neotectonics of North America*, D. E. Slemmons, E. R. Engdahl, M. D. Zoback, and D. D. Blackwell (Editors), Geological Society of America, Boulder, Colorado, 445–456.

Lewis, T. J., W. H. Bentkowski, and J. A. Wright (1991). Thermal state of the Queen Charlotte basin, British Columbia: Warm, in *Evolution and Hydrocarbon Potential of the Queen Charlotte Basin, British Columbia*, G. J. Woodsworth (Editor), *Pap. Geol. Surv. Can. 90-10*, 489–506.

Mackie, D. J., R. M. Clowes, S. A. Dehler, R. M. Ellis, and P. Morel-A-L'Huissier (1989). The Queen Charlotte Islands refraction project. Part II. Structural model for transition from Pacific plate to North American plate, *Can. J. Earth Sci.* **26,** 1713–1725.

Mazzotti, S., R. D. Hyndman, P. Flück, A. J. Smith, and M. Schmidt (2003). Distribution of the Pacific/North America motion in the Queen Charlotte Islands—S. Alaska plate boundary zone, *Geophys. Res. Lett.* **30,** doi: 10.1029/2003GL017586.

McCaffrey, R. (1994). Global variability in subduction thrust zone—Forearc systems, *Pure Appl. Geophys.* **142,** no. 1, 173–224.

Nykolaishen, L., H. Dragert, K. Wang, T. James, and M. Schmidt (2015). GPS observations of crustal deformation associated with the M_w 7.8 Haida Gwaii Earthquake, *Bull. Seismol. Soc. Am.* **105,** doi: 10.1785/0120140177.

Pollack, H. N., S. J. Hurter, and J. R. Johnson (1993). Heat flow from the Earth's interior: Analysis of the global data set, *Rev. Geophys.* **31,** 267–280, doi: 10.1029/93RG01249.

Prims, J., K. P. Furlong, K. M. M. Rohr, and R. Govers (1997). Lithospheric structure along the Queen Charlotte margin in western Canada: Constraints from flexural modeling, *Geo Mar. Lett.* **17,** 94–99.

Riedel, M., M. Côté, P. Neelands, G. Middleton, G. Standen, R. Iuliucci, M. Ulmi, C. Stacey, R. Murphy, D. Manning, C. Brillon, and G. D. Spence (2014). 2012 Haida Gwaii M_w 7.7 earthquake response—Ocean bottom seismometer relocation and geophone orientation analysis and quality control of wide-angle *P*-wave refraction data, *Geol. Surv. Canada, Open-File 7632*, 77 pp., doi: 10.4095/295551.

Ristau, J. R., G. C. Rogers, and J. F. Cassidy (2007). Stress in western Canada from regional moment tensor analysis, *Can. J. Earth Sci.* **44,** 127–148, doi: 10.1139/E06-057.

Rogers, G. C. (1982). Revised seismicity and revise fault plane solutions for the Queen Charlotte Island region, in Earth Physics Branch Open File No. 82–83, Department of Energy, Mines, and Resources, Ottawa, 77 pp.

Rogers, G. C. (1986). Seismic gaps along the Queen Charlotte fault, *Earthq. Predict. Res.* **4,** 1–11.

Rohr, K. M. M., and J. R. Dietrich (1992). Strike slip tectonics and development of the Tertiary Queen Charlotte basin, off-shore western Canada: Evidence from seismic reflection data, *Basin Res.* **4,** 1–20, doi: 10.1111/j.1365-2117.1992.tb00039.x.

Rohr, K. M. M., M. Scheidhauer, and A. Trehu (2000). Transpression between two warm mafic plates: The Queen Charlotte Fault revisited, *J. Geophys. Res.* **105,** 8147–8172.

Smith, A. J., R. D. Hyndman, J. F. Cassidy, and K. Wang (2003). Structure, seismicity, and thermal regime of the Queen Charlotte Transform margin, *J. Geophys. Res.* **108,** no. B11, 2539, doi: 10.1029/2002JB002247.

Smith, R. A. J. (1999). Structure, deformation and thermal regime of the Queen Charlotte Transform Margin, *Master's thesis*, Sch. of Earth and Ocean Sci., Univ. of Victoria, Victoria, 179 pp.

Spence, G. D., and D. T. Long (1995). Transition from oceanic to continental crustal structure: Seismic and gravity models at the Queen Charlotte transform margin, *Can. J. Earth Sci.* **32,** 699–717.

Spinelli, G. A., and K. Wang (2008). Effects of fluid circulation in subducting crust on Nankai margin seismogenic zone temperatures, *Geology* **36,** 887–890.

Stein, C. A., and S. Stein (1992). A model for the global variation in oceanic depth and heat flow with lithospheric age, *Nature* **359,** 123–129.

Wada, I., and K. Wang (2009). Common depth of slab-mantle decoupling: Reconciling diversity and uniformity of subduction zones, *Geochem. Geophys. Geosyst.* **10,** Q10009, doi: 10.1029/2009GC002570.

Wang, K. (2004). Applying fundamental principles and mathematical models to understand processes and estimate parameters, in *Hydrogeology of the ocean lithosphere*, E. E. Davis and H. Elderfield (Editor), Cambridge University Press, New York, 376–413.

Wang, K., and S. Bilek (2014). Invited review paper: Fault creep caused by subduction of rough seafloor relief, *Tectonophysics* **610,** 1–24.

Wang, K., and E. E. Davis (1992). Thermal effect of marine sedimentation in hydrothermal active areas, *Geophys. J. Int.* **110,** 70–78.

Wang, K., and K. Suyehiro (1999). How does plate coupling affect crustal stresses in northeast and southwest Japan? *Geophys. Res. Lett.* **26,** 2307–2310, doi: 10.1029/1999GL900528.

Wang, K., R. D. Hyndman, and M. Yamano (1995). Thermal regime of the southwest Japan subduction zone: Effects of age history of the subducting plate, *Tectonophys.* **248,** 53–69.

Wessel, P., and W. H. F. Smith (1995). New version of the Generic Mapping Tools released, *Eos Trans. AGU* **76,** 329.

Wilson, D. S. (1988). Tectonic history of the Juan de Fuca Ridge over the last 40 million years. *J. Geophys. Res.* **93,** 11,863–11,876.

Yorath, C. J., and R. D. Hyndman (1983). Subsidence and thermal history of Queen Charlotte Basin, *Can. J. Earth Sci.* **20,** 135–159.

Pacific Geoscience Centre
Geological Survey of Canada
Natural Resources Canada
9860 West Saanich Road
Sidney, British Columbia
Canada V8L 4B2
(K.W., J.H., R.D.H., M.R.)

Friedrich Schiller University of Jena
Institute of Geosciences
Burgweg 11
07749 Jena, Germany
(F.S.)

Manuscript received 25 June 2014